

TABLE IV. Molecular constants of tropolone.^a

Constant	Rotational ^b	Total ^c	Unit
0⁺ state			
<i>A</i>	2743.090(41)	2743.0931(54)	MHz
<i>B</i>	1659.893(15)	1659.8893(21)	MHz
<i>C</i>	1034.383 18(62)	1034.383 65(22)	MHz
Δ_J	12.55(29)	12.78(24)	Hz
Δ_{JK}	85.5(81)	82.5(60)	Hz
Δ_K	948.(54)	940.(33)	Hz
0⁻ state			
<i>A</i>	2742.650(66)	2742.7181(114)	MHz
<i>B</i>	1659.891(26)	1659.8633(30)	MHz
<i>C</i>	1034.324 14(75)	1034.324 66(54)	MHz
Δ_J	12.81(45)	13.11(36)	Hz
Δ_{JK}	84.(14)	74.8(98)	Hz
Δ_K	949.(90)	994.(56)	Hz
Δ_0	29 288.(88)	29 193.788(26)	MHz
<i>F</i>	16.391(78)	16.456(15)	MHz

^aThe figures in the parentheses are uncertainties (3σ) to be attached to the last digit. δ_J and δ_K are set to zero.

^bPure-rotational transitions observed by microwave spectroscopy were analyzed.

^cAll the transitions observed by microwave and FTMW spectroscopy were analyzed.

malonaldehyde.^{23–27} A detailed description of the interaction term will be found in a later section (Sec. V C), Eqs. (8)–(15).

Wang-type symmetric top basis functions $|0^\pm, J, K_a, M, \pm\rangle$, defined by

$$|0^\pm, J, K_a, M, \pm\rangle = (1/2)^{1/2} \{ |J, K_a, M\rangle \pm |J, -K_a, M\rangle \} |0^\pm\rangle \quad (5)$$

were used to evaluate the matrix elements, where $|0^\pm\rangle$ are the wave functions for the tunneling motion. Nonvanishing matrix elements of the interaction term H_{int} , which are off diagonal with respect to the tunneling states 0^+ and 0^- , are

$$\begin{aligned} \langle 0^+, J, K_a, M, + | H_{\text{int}} | 0^-, J, K_a \pm 1, M, - \rangle \\ = \langle 0^+, J, K_a, M, - | H_{\text{int}} | 0^-, J, K_a \pm 1, M, + \rangle \\ = F(K_a \pm 1/2) \{ J(J+1) - K_a(K_a \pm 1) \}^{1/2}, \end{aligned} \quad (6)$$

with hermiticity implied. The energy eigenvalues were calculated by direct diagonalization of the energy matrices.

A. Rotational spectrum

The observed pure-rotational transition frequencies were subjected to a least squares analysis, in which the centrifugal distortion constants δ_J and δ_K were fixed at zero. The optimized constants are listed in the second column of Table IV with uncertainties (3σ) in parentheses. The standard deviation of the fit was about 27 kHz, consistent with the experimental accuracy.

Transitions conspicuously perturbed by the tunneling-rotation interaction are given in Table I. Columns $\Delta\nu$ of this table give the transition frequencies calculated with the optimized constants in the second column of Table IV minus those calculated with the interaction constant F set to zero

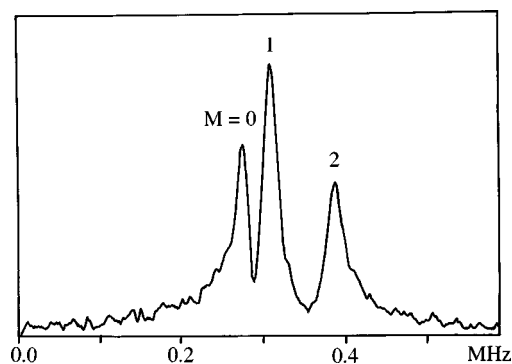


FIG. 7. The $3_{2,2}-2_{2,1}$ rotational transition in the 0^+ state observed by FTMW spectroscopy split into three ($M=0, 1,$ and 2) Stark components with the electric field of $E=4.20$ V/cm. The abscissa represents the offset from 8082.140 MHz.

and all other constants unaltered. They indicate how much the spectrum is influenced by the tunneling-rotation interaction.

B. Tunneling-rotation spectrum

The tunneling-rotation transitions in Table II were combined in a least-squares analysis with the rotational transitions in the 0^+ and 0^- states as well as newly observed 12 rotational lines in Table III. The FTMW data were weighted by unity whereas the microwave data were weighted by 0.10–0.25, referring to their relative experimental accuracies.

The determined rotational constants and the centrifugal distortion constants (Δ_J , Δ_{JK} , and Δ_K) are listed in the third column of Table IV, together with the tunneling splitting Δ_0 and the interaction constant F with uncertainties (3σ) in parentheses. Two centrifugal distortion constants δ_J and δ_K were fixed to be zero. The standard deviation of the fit was 14 kHz, consistent with the experimental accuracy. The last columns of Tables II and III show the shifts of the transition frequencies by the tunneling-rotation interaction as calculated in a similar way to the case of Table I.

C. Stark effect

The Stark effect was measured with the FTMW system for the two rotational lines $3_{2,1}-2_{2,0}$ and $3_{2,2}-2_{2,1}$ by applying a dc electric field up to 500 V between the mesh electrodes. The $3_{2,2}-2_{2,1}$ spectrum recorded under the electric field of 4.20 V/cm is split into three ($M=0, 1,$ and 2) components, as illustrated in Fig. 7. The shifts plotted against the square of the applied voltage indicate the second-order Stark effect. The spacing between the electrodes was calibrated to be 23.744 ± 0.020 cm by observing the $J=1-0$ rotational line of OC^{34}S .²⁸ The derived dipole moments along the a axis are summarized in Table V.

V. DISCUSSION

A. Molecular constants

The optimized molecular constants in the ground state are listed in Table IV. One of the most important results is